Inorg. Chem. **1994**, *33*, 665–669

Reactivity of a Chelated Phosphate Ester

James A. Connolly, Mariusz Banaszczyk, Rosemary C. Hynes, and Jik Chin*

Department of Chemistry, McGill University, Montreal, Canada H3A 2K6

Received August 11, 1993®

Hydroxyethyl phosphate forms a monodentate complex with $[(tren)Co(OH_2)_2]^{3+}$ whereas it forms a bidentate complex with $[(trpn)Co(OH_2)_2]^{3+}$ (tren = tris(2-aminoethyl)amine; trpn = tris(3-aminopropyl)amine). The monodentate phosphate hydrolyzes more rapidly ($k = 2 \times 10^{-5}$ s^{-1} at pH 6.0, 60 °C) than the bidentate phosphate. Although the chelated phosphate is highly resistant to hydrolysis, it is rapidly hydrolyzed by additional $[(trpn)Co(OH_2)_2]^{3+}$ ($k = 1 \times 10^{-2}$ M^{-1} s^{-1} at pH 6.0, 25 °C).

Over the years there has been much interest in understanding the role of metal ions in hydrolyzing phosphate esters. One important question is whether four-membered-ring metal–phosphate ester chelates could exist and play a key role in enzymic or nonenzymic systems.[1-5] There has been considerabe debate whether strain in the four-membered-ring chelates can induce rapid exocyclic hydrolysis of the ester group much like in the hydrolysis of five-membered-ring organic phosphates.[6] Although chelated metal complexes of carboxylate ions and inorganic phosphate have been prepared, syntheses of chelated phosphate monoester complexes have proven to be far more challenging. An extensive search of the Cambridge Structural Database for chelated phosphate esters turned up empty.[4] This difficulty in synthesis of chelated phosphate esters implied that such chelates might be particularly reactive and therefore worth pursuing further.[1] We recently reported that **1** efficiently hydrolyzes phosphate monoesters under mild conditions while **2** does not.[7] **1**-promoted hydrolysis of phosphate monoesters results in formation of a doubly chelated phosphate complex (**3**). Here we report on the reactivity of a phosphate monoester chelated to **1** and the crystal structure of **3**.

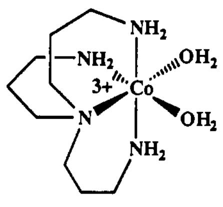

1

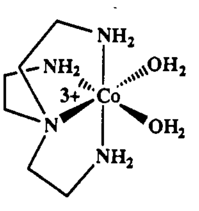

2

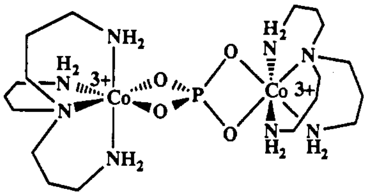

3

Experimental Section

Instruments. ^{1}H NMR (299.3 MHz), ^{31}P NMR (121.4 MHz), and ^{13}C NMR (75.4 MHz) spectra were obtained with a Varian XL-300 FT spectrometer. All spectra were recorded in D_2O with chemical shifts reported in ppm and with 3-(trimethylsilyl)-1-propanesulfonic acid (0 ppm), trimethyl phosphate (0 ppm), and dioxane (67.4 ppm) used as references for ^{1}H, ^{31}P, and ^{13}C NMR, respectively.

Materials. Tris(aminoethyl)amine (tren) was purchased from Aldrich. Tris(aminopropyl)amine (trpn) and the disodium salt of hydroxyethyl phosphate (HEP) were prepared according to published procedures.[8]

$[(trpn)Co(CO_3)]ClO_4$. The cobalt carbonato complex was prepared by a procedure using lead oxide.[9] The tetraamine ligand (50 mmol) dissolved in water (100 mL) was added to a stirring solution of $Co(ClO_4)_2$ (50 mmol) in water (250 mL). To the reaction mixture was added an aqueous solution (150 mL) of sodium bicarbonate (100 mmol) followed by PbO_2 (105 mmol). The resulting suspension was stirred vigorously for 2 days, after which 70% perchloric acid (50 mmol) was added slowly. After filtration, the volume of the filtrate was reduced *in vacuo*. The product precipitated as fine crystals. The tren complex was prepared by an analogous method. $[(trpn)Co(CO_3)]ClO_4$: ^{13}C NMR δ 167.84 (CO_3), 58.57, 56.39, 38.75, 37.86. Anal. Calcd for $C_{10}H_{24}ClCoN_4O_7$: C, 29.53; H, 5.95; N, 13.78; Cl, 8.72; Co, 14.49. Found: C, 29.73; H, 6.22; N, 13.86; Cl, 9.06; Co, 14.55.

$[(trpn)Co(OH_2)_2](ClO_4)_3$ (1). The cobalt carbonato complex was converted to the corresponding diaqua complex by adding 70% perchloric acid (2.5 equiv) to the finely ground carbonato complex. The resulting mixture was stirred under a water aspirator for 2 h. The solution was then diluted with water and the mixture freeze-dried. The resulting pink solid was washed with ether and dried in vacuo over P_2O_5. The tren complex was prepared by an analogous method.[10] $[(trpn)Co(OH_2)_2](ClO_4)_3 \cdot 2H_2O$: ^{13}C NMR δ 61.67, 57.44, 38.15, 37.58, 24.20, 22.63. Anal. Calcd for $C_9H_{28}Cl_3CoN_4O_{12}$: C, 17.5; H, 5.22; N, 9.07; Cl, 17.22; Co, 9.54. Found: C, 17.65; H, 5.62; N, 9.15; Cl, 17.10; Co, 9.77.

$\{[(trpn)Co]_2(\mu_4\text{-}PO_4)\}(ClO_4)_3$ (3). To a freshly prepared solution of **1** (4 mmol) in water (50 mL) was added a solution of Na_2HPO_4 (2 mmol) in water (25 mL) and the pH adjusted to 4 with 0.1 N NaOH. $NaClO_4$ was then added to induce crystallization. The resulting product was further recrystallized from aqueous $NaClO_4$: ^{13}C δ NMR 58.72, 58.43, 56.24, 38.39, 37.45, 37.30, 23.96, 21.63, 21.44; ^{31}P NMR δ 40.5. Anal. Calcd for $C_{18}H_{48}N_8Cl_3Co_2O_{16}P$: C, 24.35; H, 5.48; N, 12.62; Cl, 11.98; Co, 13.28; P, 3.49. Found: C, 24.52; H, 5.38; N, 12.63; Cl, 12.12; Co, 13.48; P, 3.48.

X-ray Diffraction Studies of 3. All measurements were carried out using Mo Kα radiation (0.710 69 Å) with a graphite-crystal, incident-beam monochromator on a Rigaku AFC6S diffractometer controlled by TEXRAY[11] software. The ω-scan mode was used. All calculations for

---

® Abstract published in *Advance ACS Abstracts*, January 1, 1994.

(1) Hendry, P.; Sargeson, A. M. *J. Am. Chem. Soc.* **1989**, *111*, 2521.

(2) Anderson, B.; Milburn, R. M.; Harrowfield, J. MacB.; Robertson, G. B.; Sargeson, A. M. *J. Am. Chem. Soc.* **1977**, *99*, 2652.

(3) Cooperman, B. S. In *Metal Ions in Biological Systems*; Sigel, H., Ed.; Dekker: New York, 1976; Vol. 5, pp 80–125.

(4) Alexander, R. S.; Kanyo, Z. F.; Chirlian, L. E.; Christianson, D. W. *J. Am. Chem. Soc.* **1990**, *112*, 933.

(5) Spiro, T. G.; Farrell, F. J.; Kjellstrom, W. A. *Science (Washington, D.C.)* **1969**, *164*, 320.

(6) Westheimer, F. H. *Acc. Chem. Res.* **1967**, *1*, 70.

(7) Chin, J.; Banaszczyk, M. *J. Am. Chem. Soc.* **1989**, *111*, 4103–4105.

(8) Chin, J.; Banaszczyk, B.; Jubian, V.; Zou, X. *J. Am. Chem. Soc.* **1989**, *111*, 186.

(9) Loehlin, J. H.; Fleisher, E. B. *Acta Crystallogr.* **1976**, *B32*, 3063.

(10) Harris, G. M.; Dasgupta, T. P. *J. Am. Chem. Soc.* **1975**, *97*, 1733.

(11) TEXRAY Structure Analysis Package, Molecular Structure Corp., Houston, TX.

0020-1669/94/1333-0665$04.50/0

Table 1. Crystallographic Data for $\{[(\text{trpn})\text{Co}]_2(\mu_4\text{-PO}_4)\}(\text{ClO}_4)_3(\text{H}_2\text{O})_3$

mol formula	$C_{18}H_{42}N_8O_{19}PCl_3Co_2$
mol wt	929.77
cryst dimens, mm	0.40 × 0.15 × 0.08
temp, °C	20 ± 1
linear abs coeff, mm^{-1}	1.23
h, k, l limits	−8 to 8, 0 to 19, 0 to 26
2θ range, deg	5–45
F(000)	1911.63
no. of data collected	5280
no. of unique data	4879
no. of data with $I > 2.5\sigma(I)$	2794
no. of variables	466
largest shift/esd in final cycle	0.114
weight modifier "*w*"	5.0×10^{-4}
R^a	0.082
$R_w{}^b$	0.108
goodness of fit^c	2.22

[a] $R = \sum(F_o - F_c)/\sum F_o$. [b] $R_w = \{\sum[w(F_o - F_c)^2]/\sum wF_o^2\}^{1/2}$. [c] $\text{GoF} = \{\sum[w(F_o - F_c)^2]/(\text{no. of reflns} - \text{no. of params})\}^{1/2}$.

Table 2. Atomic Parameters and B_{eq} Values[a]

	x	*y*	*z*	B_{eq}, Å^2
Co(1)	0.43390(23)	0.61731(10)	0.33388(7)	2.02(8)
Co(2)	0.62123(23)	0.62000(10)	0.14938(7)	1.93(8)
P	0.5472(5)	0.62112(19)	0.24497(14)	2.89(16)
O(1)	0.5044(12)	0.5552(4)	0.2782(3)	2.4(4)
O(2)	0.5261(12)	0.6835(5)	0.2846(4)	2.9(4)
O(3)	0.4363(11)	0.6299(5)	0.1890(3)	2.1(4)
O(4)	0.7187(11)	0.6168(5)	0.2274(3)	2.8(4)
N(1)	0.3508(15)	0.5368(6)	0.3774(5)	3.1(6)
N(2)	0.2194(15)	0.6289(6)	0.2875(5)	3.3(6)
N(3)	0.6540(14)	0.6132(6)	0.3785(4)	2.6(5)
N(4)	0.3843(15)	0.7025(6)	0.3760(4)	2.9(6)
N(5)	0.4886(14)	0.6280(6)	0.0754(4)	2.7(5)
N(6)	0.5970(13)	0.5130(6)	0.1507(4)	2.5(5)
N(7)	0.6648(14)	0.7255(6)	0.1519(4)	2.5(6)
N(8)	0.8393(13)	0.6050(6)	0.1295(4)	2.7(5)
C(1)	0.192(3)	0.5034(11)	0.3476(7)	6.7(11)
C(2)	0.1618(24)	0.4967(10)	0.2905(7)	5.7(10)
C(3)	0.1422(18)	0.5644(8)	0.2579(6)	3.5(8)
C(4)	0.4688(23)	0.4748(9)	0.3821(7)	5.2(9)
C(5)	0.6407(20)	0.4868(9)	0.4068(7)	4.5(9)
C(6)	0.7382(20)	0.5412(8)	0.3825(6)	3.7(7)
C(7)	0.321(3)	0.5604(10)	0.4317(7)	6.3(11)
C(8)	0.248(3)	0.6293(9)	0.4404(7)	5.5(11)
C(9)	0.3324(22)	0.6944(9)	0.4303(6)	4.6(9)
C(10)	0.3966(19)	0.5600(8)	0.0567(6)	3.5(7)
C(11)	0.3101(19)	0.5256(8)	0.1006(6)	3.6(7)
C(12)	0.4287(20)	0.4828(8)	0.1424(6)	3.7(8)
C(13)	0.3567(18)	0.6868(8)	0.0758(6)	3.3(7)
C(14)	0.4134(22)	0.7647(8)	0.0894(7)	4.3(8)
C(15)	0.5174(22)	0.7715(8)	0.1454(6)	3.9(8)
C(16)	0.5861(18)	0.6478(8)	0.0305(6)	3.3(7)
C(17)	0.7352(20)	0.6021(8)	0.0302(6)	3.6(7)
C(18)	0.8744(18)	0.6236(8)	0.0728(6)	3.3(7)

[a] Esd's refer to the last significant digits. B_{eq} is the mean of the principal axes of the thermal ellipsoid for atoms refined anisotropically.

Table 3. Bond Distances (Å)

Co(1)–O(1)	1.953(8)	N(3)–C(6)	1.492(19)
Co(1)–O(2)	1.963(9)	N(4)–C(9)	1.488(19)
Co(1)–N(1)	2.018(11)	N(5)–C(10)	1.498(18)
Co(1)–N(2)	1.964(12)	N(5)–C(13)	1.536(19)
Co(1)–N(3)	1.973(11)	N(5)–C(16)	1.519(17)
Co(1)–N(4)	1.963(11)	N(6)–C(12)	1.479(19)
Co(2)–O(3)	1.950(8)	N(7)–C(15)	1.469(20)
Co(2)–O(4)	1.980(9)	N(8)–C(18)	1.523(17)
Co(2)–N(5)	1.991(11)	C(1)–C(2)	1.41(3)
Co(2)–N(6)	1.979(11)	C(2)–C(3)	1.481(24)
Co(2)–N(7)	1.972(10)	C(4)–C(5)	1.47(3)
Co(2)–N(8)	1.957(10)	C(5)–C(6)	1.472(22)
P–O(1)	1.540(9)	C(7)–C(8)	1.43(3)
P–O(2)	1.541(9)	C(8)–C(9)	1.427(25)
P–O(3)	1.548(9)	C(10)–C(11)	1.532(21)
P–O(4)	1.546(10)	C(11)–C(12)	1.528(22)
N(1)–C(1)	1.528(22)	C(13)–C(14)	1.529(22)
N(1)–C(4)	1.490(20)	C(14)–C(15)	1.521(23)
N(1)–C(7)	1.475(20)	C(16)–C(17)	1.490(22)
N(2)–C(3)	1.486(18)	C(17)–C(18)	1.487(22)

solution and refinement were performed on a Vaxstation 3520 computer using the NRCVAX[12] crystallographic software. A purple multifaceted crystal was sealed in a glass capillary tube with a drop of mother liquor present to prevent dehydration. Lattice parameters for **3** were determined by least-squares refinement using the setting angles of 20 reflections in the range $16.00 < 2\theta < 27.00°$. Data were collected to a maximum 2θ of 45.00°. The cell is monoclinic, space group $P2_1/c$, with dimensions $a = 8.2415(24)$ Å, $b = 18.399(3)$ Å, $c = 24.868(4)$ Å, $\beta = 99.085(18)°$, and $V = 3723.7(14)$ Å^3, with $Z = 4$ and $\rho_{calcd} = 1.658$ g/cm^3. Absorption correction from four ψ scans was applied with transmission factors ranging from 0.586 to 0.759. The structure was solved by direct methods followed by a difference Fourier analysis. Hydrogen positions were calculated. The structure was refined with all non-hydrogen atoms anisotropic except the partial-occupancy oxygens of the disorderd perchlorate and water molecule. Protons on the water molecules were omitted. The crystal structure consists of a dimeric cation plus three perchlorate ions and three water molecules of solvation per asymmetric unit. The final cycle of full-matrix least-squares refinement was based on 2794 observed reflections ($I > 2.5\sigma(I)$) and 466 variable parameters and converged with agreement factors of $R = 0.082$ and $R_w = 0.103$. The disorder in the perchlorate anions resulted in the poor residuals. The deepest hole in the final difference map was −0.960 e Å^{-3} and the largest peak was 1.630 e Å^{-3}, near the disordered perchlorate. Results are summarized in Tables 1–4 and Figure 2.

Equilibrium. Complexation of HEP (0.025–0.1 M) to **1** and **2** (0.025–0.1 M) in D_2O at pD 6.0 and 25 °C was monitored by ^{31}P NMR. The NMR spectra in Figure 1 were taken with an aquisition temperature and time of 20 °C and 300 min, respectively, after incubating the samples for approximately 1 h at 20 °C.

Kinetics. Cobalt complex promoted hydrolysis of HEP in D_2O at pD 6.0 was monitored by following the increase in the ^{1}H NMR signal due to ethylene glycol production. Cobalt complex **2** (0.05 M) promoted hydrolysis of HEP (0.025–0.1 M) was monitored at 60 °C for about 24 h. The pseudo-first-order rate constant for hydrolysis of HEP coordinated to **2** was obtained by dividing the initial rate of ethylene glycol production by the concentration of HEP coordinated to **2** as determined by ^{31}P NMR. Each kinetic run was reproducible to within 15% error. Cobalt complex **1** (0.05 M) did not hydrolyze HEP (0.1 M) to an observable extent (at 60 °C for 2 days) when excess HEP was used. Hydrolysis of HEP (0.025 M) with excess **1** (0.05–0.125 M) was monitored to completion at 25 °C within minutes to hours.

Results and Discussion

Binding. The first chelated phosphate monoester of a cobalt(III) complex (**4**) was thought to have been synthesized in 1977.[2] However, ^{31}P NMR and ultimately X-ray crystallography revealed that the cobalt complex is a phosphate ester bridged dimer (**5**).[13] Over the years, attempts at synthesis and isolation of chelated phosphate esters have proven fruitless.[1] As shown below, chelated phosphate monoesters cannot be synthesized from just any octahedral cobalt complex of the type *cis*-$[\text{Co(N}_4)(\text{OH}_2)_2]^{3+}$ where N_4 represents a tetraamine ligand. The

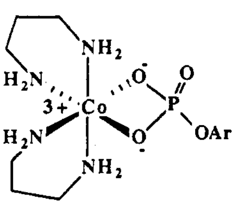

4

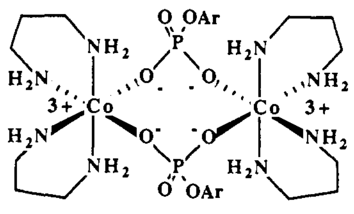

5

---

[12] NRCVAX: Gabe, E. J.; LePage, Y.; Charland, J. P.; Lee, F. L.; White, P. S. *J. Appl. Crystallogr.* **1989**, *22*, 384–387.

[13] (a) Jones, D. R.; Lindoy, L. F.; Sargeson, A. M. *J. Am. Chem. Soc.* **1984**, *106*, 7807. (b) Jones, D. R.; Lindoy, L. F.; Sargeson, A. M.; Snow, M. R. *Inorg. Chem.* **1982**, *21*, 4155.

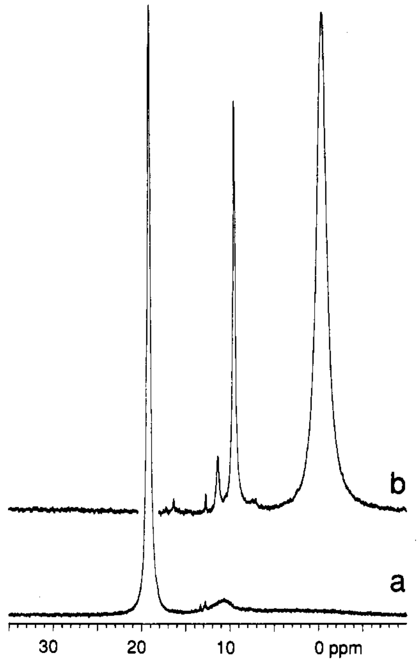

Figure 1. ^{31}P NMR spectra showing the complexation of hydroxyethyl phosphate (0.15 M) to (a) **1** (0.15 M) and (b) **2** (0.15 M).

Table 4. Bond Angles (deg)

O(1)–Co(1)–O(2)	74.5(3)	Co(2)–O(3)–P	92.7(4)
O(1)–Co(1)–N(1)	96.6(4)	Co(2)–O(4)–P	91.6(4)
O(1)–Co(1)–N(2)	89.3(4)	Co(1)–N(1)–C(1)	111.8(9)
O(1)–Co(1)–N(3)	91.5(4)	Co(1)–N(1)–C(4)	109.3(9)
O(1)–Co(1)–N(4)	162.8(4)	Co(1)–N(1)–C(7)	113.2(10)
O(2)–Co(1)–N(1)	171.1(4)	C(1)–N(1)–C(4)	103.2(13)
O(2)–Co(1)–N(2)	88.1(5)	C(1)–N(1)–C(7)	108.0(13)
O(2)–Co(1)–N(3)	87.9(4)	C(4)–N(1)–C(7)	110.9(13)
O(2)–Co(1)–N(4)	88.3(4)	Co(1)–N(2)–C(3)	118.7(9)
N(1)–Co(1)–N(2)	92.6(5)	Co(1)–N(3)–C(6)	116.6(9)
N(1)–Co(1)–N(3)	91.7(5)	Co(1)–N(4)–C(9)	121.2(9)
N(1)–Co(1)–N(4)	100.6(5)	Co(2)–N(5)–C(10)	113.7(8)
N(2)–Co(1)–N(3)	175.6(5)	Co(2)–N(5)–C(13)	109.4(8)
N(2)–Co(1)–N(4)	89.0(5)	Co(2)–N(5)–C(16)	114.8(9)
N(3)–Co(1)–N(4)	88.9(5)	C(10)–N(5)–C(13)	105.5(11)
O(3)–Co(2)–O(4)	74.7(4)	C(10)–N(5)–C(16)	105.9(10)
O(3)–Co(2)–N(5)	95.8(4)	C(13)–N(5)–C(16)	107.1(10)
O(3)–Co(2)–N(6)	89.7(4)	Co(2)–N(6)–C(12)	117.8(9)
O(3)–Co(2)–N(7)	92.6(4)	Co(2)–N(7)–C(15)	114.9(9)
O(3)–Co(2)–N(8)	164.3(4)	Co(2)–N(8)–C(18)	121.2(9)
O(4)–Co(2)–N(5)	170.4(4)	N(1)–C(1)–C(2)	121.8(15)
O(4)–Co(2)–N(6)	88.9(4)	C(1)–C(2)–C(3)	117.7(16)
O(4)–Co(2)–N(7)	87.4(4)	N(2)–C(3)–C(2)	113.6(13)
O(4)–Co(2)–N(8)	89.8(4)	N(1)–C(4)–C(5)	119.5(14)
N(5)–Co(2)–N(6)	92.7(4)	C(4)–C(5)–C(6)	118.9(14)
N(5)–Co(2)–N(7)	91.5(4)	N(3)–C(6)–C(5)	110.6(12)
N(5)–Co(2)–N(8)	99.8(5)	N(1)–C(7)–C(8)	122.3(15)
N(6)–Co(2)–N(7)	174.9(5)	C(7)–C(8)–C(9)	119.3(16)
N(6)–Co(2)–N(8)	87.9(5)	N(4)–C(9)–C(8)	117.5(13)
N(7)–Co(2)–N(8)	88.7(5)	N(5)–C(10)–C(11)	113.2(11)
O(1)–P–O(2)	100.6(5)	C(10)–C(11)–C(12)	112.2(13)
O(1)–P–O(3)	114.3(5)	N(6)–C(12)–C(11)	112.7(12)
O(1)–P–O(4)	114.1(5)	N(5)–C(13)–C(14)	118.1(12)
O(2)–P–O(3)	112.8(5)	C(13)–C(14)–C(15)	112.8(12)
O(2)–P–O(4)	114.8(5)	N(7)–C(15)–C(14)	113.0(12)
O(3)–P–O(4)	100.8(5)	N(5)–C(16)–C(17)	113.7(12)
Co(1)–O(1)–P	92.2(4)	C(16)–C(17)–C(18)	112.9(12)
Co(1)–O(2)–P	91.8(4)	N(8)–C(18)–C(17)	111.2(11)

equilibrium constant for chelation of phosphate monoesters to *cis*-$[Co(N_4)(OH_2)_2]^{3+}$ is highly sensitive to the structure of the N_4 tetraamine ligand. While **1** forms phosphate monoester chelates almost exclusively, **2** does not form any such chelates.

Complexation of hydroxyethyl phosphate (HEP) to **1** (Figure 1a) and **2** (Figure 1b) was monitored by ^{31}P NMR. There are two striking differences between spectra a and b of Figure 1. First, the chemical shift due to HEP coordinated to **1** (δ 19.2 ppm) is about twice that of HEP coordinated to **2** (δ 9.6 ppm). Second, the intensity of the peak due to HEP coordinated to **1** is much greater than that due to HEP coordinated to **2**. These spectral differences are caused by different modes of binding of HEP to **1** and **2**. The ^{31}P NMR signals of phosphates shift progressively downfield with increase in the number of phosphate oxygen–Co(III) bonds. Typically, phosphates with one, two, three, and four phosphate oxygen–Co(III) bonds have ^{31}P NMR chemical shifts at about δ 10, 20, 30, and 40 ppm, respectively, relative to trimethyl phosphate.[7,14] Interestingly, HEP coordinates to **2** as a monodentate ligand (**2p**) whereas it chelates to **1** as a bidentate ligand (**1p**). Acetate also coordinates to **2** as a monodentate ligand whereas it chelates to **1** as a bidentate ligand.[15] When HEP coordinates to **2**, two ^{31}P NMR signals are generated, since either of the two coordinated water molecules can be displaced. The water molecule *cis* to the primary amine should be replaced in preference to the water molecule *cis* to the more sterically bulky tertiary amine.

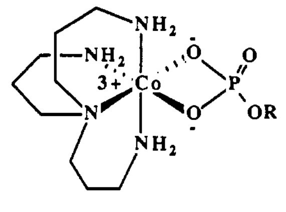

1p

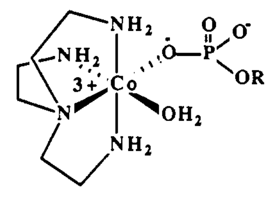

2p

The O–Co–O bond angle in **1** is expected to decrease upon formation of the four-membered-ring chelate (**1p**). From steric considerations, the N–Co–N bond angle opposite the O–C–O bond angle should increase upon formation of the four-membered-ring chelate. The N–Co–N bond angle opposite the O–Co–O bond angle in **2** is held rigidly in a five-membered ring whereas the N–Co–N bond angle in **1** is more flexible. The more flexible complex **1** favors formation of the four-membered-ring chelate with HEP. The equilibrium constant for monodentate coordination of HEP to **2** as determined by ^{31}P NMR is 10 M^{-1} (Figure 1b). In contrast, the equilibrium constant for chelation of HEP to **1** is greater than 300 M^{-1} (Figure 1a). It was previously shown[8] that **1** is close to 3 orders of magnitude more reactive than **2** for hydrolyzing phosphate diesters because of the greater flexibility of the N–Co–N bond angle in **1**, resulting in the ease of formation of four-membered-ring transition-state chelates.

Hydrolysis. Cobalt complexes **1** and **2** promoted hydrolysis of HEP was monitored by following the increase in the ^1H NMR signal due to ethylene glycol production. HEP was selected as the substrate because the ^1H NMR signal of ethylene glycol does not overlap with that of the cobalt complex. Interestingly, **1** is more reactive than **2** when excess cobalt complex is used whereas **2** is more reactive than **1** when excess HEP is used.

Excess HEP. The pseudo-first-order rate constant for hydrolysis of HEP coordinated to **2** at pH 6.0 and 60 °C is 2×10^{-5} s^{-1}. Under the same experimental conditions, HEP chelated to **1** does not hydrolyze to any observable extent. Therefore, **2** is far more reactive than **1** when excess HEP is used. It has been shown that large rate acceleration for phosphate monoester hydrolysis can be obtained by joint Lewis acid activation and metal–hydroxide activation.[16] Such a double-activation path is available for **2** but not for **1**. These studies reveal that a greater rate acceleration can be obtained by joint Lewis acid activation and metal–hydroxide activation than by chelation.

It is interesting to compare the rates of **1**- and **2**-promoted hydrolysis of phosphate monoesters to those of **1**- and **2**-promoted

---

(14) Haight, G. P., Jr. *Coord. Chem. Rev.* **1987**, *79*, 293.
(15) Chin, J.; Banaszczyk, M. *J. Am. Chem. Soc.* **1989**, *111*, 2724.
(16) Jones, D. R.; Lindoy, L. F.; Sargeson, A. M. *J. Am. Chem. Soc.* **1983**, *105*, 7327.

hydrolysis of phosphate diesters.[8] In contrast to the phosphate monoester results, **1** is far more reactive than **2** for hydrolyzing phosphate diesters. Because phosphate diesters are much less basic than phosphate monoesters, phosphate diesters coordinate to both **1** and **2** as monodentate ligands. Unlike in phosphate monoester hydrolysis, both **1** and **2** can provide joint Lewis acid activation and metal–hydroxide activation for hydrolyzing phosphate diesters. It is the ability of **1** to easily form four-membered-ring complexes that is responsible for its efficiency in hydrolyzing phosphate diesters as well as its inefficiency in hydrolyzing phosphate monoesters. In phosphate diester hydrolysis, **1** stabilizes the four-membered-ring transition state whereas in phosphate monoester hydrolysis **1** forms the four-membered-ring complex with the starting material.

Excess Cobalt Complex. Although HEP chelated to **1** is stable, it is rapidly hydrolyzed when excess **1** is added to the chelated complex. The second-order rate constant for **1**-promoted hydrolysis of HEP chelated to **1** is 1×10^{-2} M^{-1} s^{-1} at 25 °C. In contrast, **2** does not hydrolyze HEP by a bimetallic path. When excess cobalt complex is used, **1** is far more efficient than **2** for hydrolyzing HEP. Hydrolysis of HEP (0.025 M) is complete within 40 min at 25 °C and pH 6 when excess **1** (0.125 M) is used. Interestingly, other *cis*-diaqua metal complexes such as **6** efficiently hydrolyze HEP chelated to **1** (1×10^{-3} M^{-1} s^{-1} at 40 °C). Monoaqua metal complexes like [Cu(diene)OH$_2$]$^{2+}$ or [Cu(terpy))H$_2$O]$^{2+}$ do not hydrolyze HEP chelated to **1** (diene = diethylenetriamine; terpy = terpyridyl). The copper complex (**6**) by itself, even when added in excess, does not hydrolyze HEP at an observable rate. Therefore HEP chelated to **1** is more susceptible to hydrolysis than free HEP. We propose that **1** hydrolyzes HEP by triple Lewis acid activation and metal–hydroxide activation (**7**), resulting in formation of the doubly chelated phosphate (**3**). Similarly, **6** hydrolyzes HEP chelated to **1** by triple Lewis acid activation and metal–hydroxide activation (**8**). The equilibrium constant for formation of **7** from the chelated HEP (**1p**) and **1** is too small to be detected ($K < 1$ M^{-1}). Since the second-order rate constant for **1**-promoted hydrolysis of **1p** is 1×10^{-2} M^{-1} s^{-1}, the pseudo-first-order rate constant for hydrolysis of HEP in **7** should be greater than 1×10^{-2} s^{-1} (at 25 °C). Outside the realm of enzymes, this represents by far the greatest rate acceleration for phosphate monoester hydrolysis. The pseudo-first-order rate constant for methyl phosphate hydrolysis in the absence of any catalyst is 2×10^{-10} s^{-1} at pH 6 and 25 °C.[17]

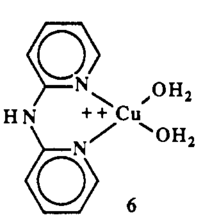

6

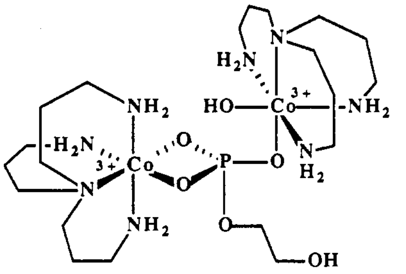

7

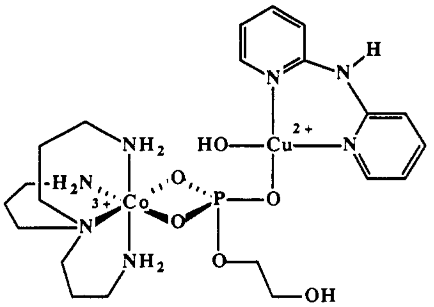

8

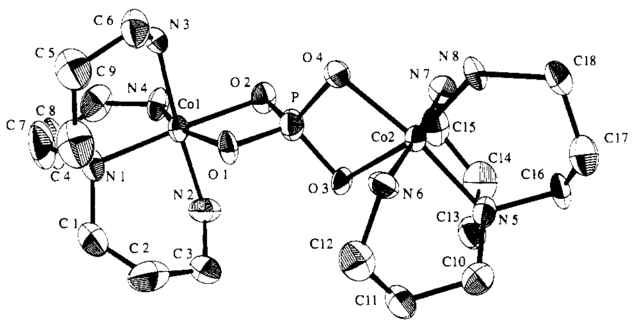

Figure 2. ORTEP[19] plot of the binuclear structure of **3**. Thermal ellipsoids are shown at 50% probability.

It is interesting to note that **2** does not hydrolyze HEP by a bimetallic path. Clearly, the equilibrium constant for formation of **9** and **2** from **2p** should be greater than that for formation of **7** from **1** and **1p**.[18] However, the only additional activation that the second cobalt complex in **9** can provide is Lewis acid activation since an intramolecular metal hydroxide group is already present in the first cobalt complex. In contrast, the second cobalt complex in **7** can provide both Lewis acid and metal–hydroxide activation.

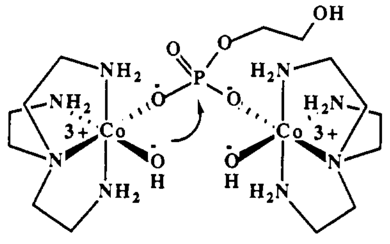

9

Binuclear Structure. Although there is no plane of symmetry in **3**, the two cobalt centers are superimposable by two rotations. Therefore there are nine distinct carbon centers in **3**, giving nine ^{13}C NMR signals. The crystal structure of the binuclear complex is shown in Figure 2. This structure reveals some valuable and interesting insights into the structural requirements of a binuclear metal complex for hydrolyzing phosphate monoesters. First, two *cis*-diaqua metal complexes that easily form four-membered rings are needed. Second, the two *cis*-diaqua metal complexes should be arranged *perpendicular* to one another as in **3**. This is indicated by the 89.2° dihedral angle between the two four-membered rings in **3**. It is interesting that **1** like purple acid phosphatases (PAP) hydrolyzes phosphate monoesters efficiently by a bimetallic process.[20] Different metals can be mixed in both the enzymic and the nonenzymic systems. Furthermore, both PAP and the

---

(17) Guthrie, J. P. *J. Am. Chem. Soc.* **1977**, *99*, 3991.

(18) Under our experimental conditions, **7** and **9** do not accumulate to levels that would be detectable by ^{31}P NMR.

(19) ORTEP: Johnson, C. K. (1976) ORTEP—A Fortran Thermal Ellipsoid Plot Program. Technical Report ORNL-5138; Oak Ridge National Laboratory: Oak Ridge, TN, 1976.

(20) (a) Que, L., Jr.; Scarrow, R. C. In *Metal Clusters in Proteins*; Que, L., Jr., Ed.; ACS Symposium Series 372; American Chemical Society: Washington, DC, 1988; pp 152–178. (b) Sage, J. T.; Xia, Y.-M.; Debrunner, P. G.; Keough, D. T.; de Jersey, J.; Zerner, B. *J. Am. Chem. Soc.* **1989**, *111*, 7239–7247 and references therein.

cobalt complex (**1**) reach maximum efficiency for hydrolyzing phosphate monoesters under mildly acidic conditions.

In conclusion, synthesis of phosphate monoesters chelated to **1** can be easily accomplished. Chelation by itself does not result in rapid hydrolysis of the phosphate monoester. Indeed, hydroxyethyl phosphate coordinated to **2** as a monodentate ligand is hydrolyzed much more rapidly than the monoester chelated to **1**. However the chelated phosphate monoester can undergo rapid hydrolysis by a bimetallic path.

Acknowledgment. Financial support of this research by the Natural Sciences and Engineering Research Council of Canada and the U.S. Army Research Office is gratefully acknowledged.

Supplementary Material Available: Tables of hydrogen atom parameters, anisotropic thermal parameters, and torsion angles and a packing diagram for $\{[(\mathrm{trpn})\mathrm{Co}]_2(\mu_4\text{-}\mathrm{PO}_4)\}(\mathrm{ClO}_4)_3$ (4 pages). Ordering information is given on any current masthead page.